Seismic design of geosynthetic-reinforced earth retaining walls following a pseudo-static approach

Seismic design of geosynthetic-reinforced earth retaining walls following a pseudo-static approach

D Gaudio[1, 2], L Masini[1] and S Rampello[1]

[1] Department of Structural and Geotechnical Engineering, Sapienza University of Rome, via Eudossiana 18, 00184 Rome, Italy
[2] present address: Department of Engineering, University of Cambridge, Trumpington Street, Cambridge, CB21PZ, UK
E-mail: dg564@cam.ac.uk

Abstract. Geosynthetic-reinforced earth (GRE) retaining walls show a better performance than conventionally-designed walls during destructive earthquakes, due to their capability of redistributing seismic-induced deformations within the reinforced zone. In this paper, a recently-proposed method to design GRE walls is first recalled, where the wall is designed to trigger an internal plastic mechanism in the presence of strong earthquakes. Following a pseudo-static approach, the seismic coefficient k is therefore assumed equal to the internal seismic resistance of the wall k_c^{int}. The seismic coefficient is then calibrated against given seismic wall performance, expressed in terms of limit values of earthquake-induced displacements. Permanent displacements are evaluated through empirical relationships that were previously developed on the basis of a parametric integration of an updated Italian seismic database. Effectiveness of the proposed procedure is then demonstrated by assessing, through Finite Difference nonlinear dynamic analyses, the seismic performance of two walls, namely a GRE and a conventional gravity wall, characterised by the same seismic resistance but triggering an internal and external plastic mechanism, respectively. They are both subjected to a real strong motion, capable of activating a plastic mechanism. Results showed that lower permanent displacements are accumulated in the GRE wall where internal mechanisms are triggered.

1. Introduction

Geotechnical systems subjected to strong earthquakes usually go beyond the elastic regime, strongly involving nonlinear and inelastic soil behaviour. Instead of trying to avoid this occurrence, one can profitably take advantage of plastic mechanisms triggered during the seismic event, provided that they are not followed by a sudden drop of system resistance, but are rather characterised by ductile stress-strain relationships. This design paradigm, the so-called *Capacity Design*, was firstly conceived for structural engineering [1] and now is increasingly adopted in the geotechnical design as well. This approach for seismic design typically leads to strongly reduce the inertial forces transmitted to the structure though accumulating permanent displacements till the end of the seismic event. In the framework of *Performance-Based Design* (PBD), safety check is then verified if these displacements are lower than given threshold values, the latter related to the considered limit state and to the design working life of the structure at hand.

The recalled concepts have been recently applied for the seismic design of geosynthetic-reinforced earth (GRE) retaining walls [2, 3], as their good performance under strong seismic loading is widely recognised from both experimental [4] and numerical analyses [5, 6], as well as from post-earthquake surveys [7]. The main reason why GRE walls behave better than conventionally-design gravity walls is

to be attributed to their capability of redistributing seismic-induced deformations into the reinforced zone, provided that reinforcement layers are adequately ductile [8], as geosynthetics usually are.

In this paper, a recently-proposed procedure to design GRE walls following a pseudo-static approach is first summarised. In this design strategy, the walls are designed to activate internal plastic mechanisms during strong ground motions, so as to involve the ductile behaviour of geosynthetic reinforcing layers. To this end, the seismic coefficient k to be used in Limit Equilibrium (LE) computations is assumed to be equal to the critical seismic coefficient related to an internal plastic mechanism, k_c^{int}, that in turn is to be lower than the ones resulting from external plastic mechanisms (e.g. sliding, bearing capacity, overturning), k_c^{ext}, so that an internal mechanism is actually involved. In order to implicitly meet the requirements of PBD in terms of displacements through LE calculations, the seismic coefficient k is then calibrated against given levels of seismic performance, here expressed in terms of threshold displacements d_y, where permanent displacements come from a parametric integration of an updated version of the Italian seismic database via the rigid-block Newmark method [9].

Validity of the proposed design procedure is demonstrated through an illustrative calculation example carried out by performing Finite Difference (FD) nonlinear dynamic analyses, through which the seismic performance of a GRE wall is compared with that of a conventional gravity wall. The two walls are characterised by the same seismic resistance (i.e. the same critical seismic coefficient k_c) but the GRE wall is designed on purpose to trigger an internal plastic mechanism, while the conventional gravity wall can activate external mechanisms only. In the analyses, the walls are subjected to the same real horizontal acceleration time history, representative of a seismic event intense enough to trigger plastic mechanisms. This calculation example validates the proposed design procedure that aims at designing GRE walls for internal plastic mechanisms.

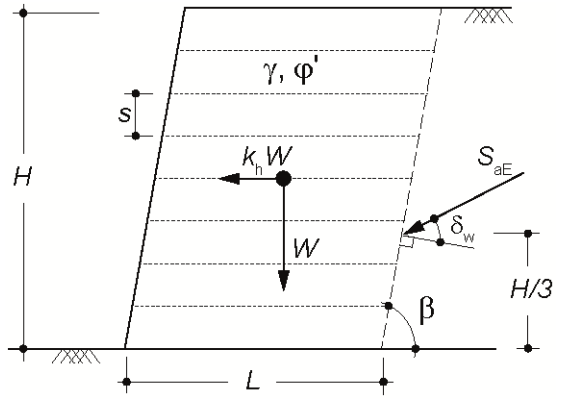

Figure 1. Layout of the problem considered in the parametric study.

Table 1. Non-dimensional parameters used in th parametric study

Parameter	Value
L/H	0.7 – 0.8 – 0.9 – 1.0
β	70° – 80°
φ′	32° – 35° – 38°
k_c	0.005 ÷ 0.300

2. Proposed design method

Problem layout considered in developing the proposed design procedure is given in figure 1. A fill of height H is retained by an earth structure with slope angle β and is reinforced by n geogrid layers, all characterised by uniform spacing s, same length L and tensile strength T_T. At the soil-geogrid contact a purely frictional strength is assumed with an angle of shearing resistance $\varphi'_{s/GSY} = \tan^{-1}(f_{s/GSY} \cdot \tan\varphi')$, where $f_{s/GSY}$ is the interface friction factor.

Following a pseudo-static approach to represent seismic-induced effects, forces acting onto the retaining wall are the self-weight W, the active earth thrust in pseudo-static conditions S_{aE} and the inertial force $k \cdot W$ acting at the centre of gravity of the wall. Preliminary studies showed that the vertical component of inertial forces does not have a remarkable influence on the semi-empirical relationships that will be used in the following to calibrate the seismic coefficient k [2]: therefore, this component is neglected in the sequel ($k_v = 0$).

Internal plastic mechanisms were first detected through the upper-bound theorem of limit analysis, finding for each system the plastic mechanism that maximises the tensile strength demand T_T to reinforcing layers (i.e. the critical plastic mechanism). A Matlab routine was implemented to this purpose, so as to find the values of geometrical parameters defining the critical mechanism (e.g. angle of inclination of a sliding planar surface). Values of the non-dimensional quantities adopted in the dimensionless parametric study are given in table 1. For the non-dimensional parameters that are not listed in table 1, the following constant values were adopted, as their influence on the strength demand turned out to be negligible: $s/H = 1/16$ and $f_{s/GSY} = 0.8$. The latter is clearly an approximation as the interface friction factor actually depends on several factors [10]. More details on the plastic mechanisms can be found in [2].

In addition to the strength demand required to geosynthetic reinforcing layers to bring the system into equilibrium, the detected plastic mechanisms provided the shape coefficient $C = d/d_0$ as well, that is defined as the ratio between the earthquake-induced horizontal permanent displacement at the toe of the wall, d, and the displacement resulting by double integrating the relative motion of a rigid block sliding on a horizontal plane, d_0 [9]. By definition, the shape coefficient takes into account the shape of the critical mechanism developing in the GRE wall for a given set of values of the non-dimensional parameters given in table 1.

Shape coefficients were then applied to obtain the corrected displacements d starting from Newmark displacement d_0, as schematically shown in figure 2. Permanent displacements d_0 were first computed through a parametric integration of an updated Italian seismic database [11], where acceleration time histories recorded during earthquakes occurred in the time frame 1972 ÷ 2017 on the Italian national territory are collected. These time traces were split up into five groups, corresponding to the five subsoil classes defined by the Italian Building Code [12]. For each group, acceleration time histories were scaled either up or down to match predefined peak acceleration values, namely $a_{max} = 0.05$, 0.15, 0.25 and $0.35g$, removing those requiring scaling factors F less than 0.5 or more than 2. Permanent displacements d_0 were then calculated through the double integration of the equation of relative motion considering both signs of accelerations and values of the ratio $k_c/k_{max} = 0.1 \div 0.8$, where $k_{max} = a_{max}/g$ is the maximum seismic coefficient of the seismic input. These displacements were therefore multiplied by the shape coefficient C to compute the corrected displacement, $d = C \cdot d_0$, and relevant upper-bound (95th percentile) semi-empirical relationships expressed through the following functional form were obtained:

$$d = B_{1c} \cdot e^{-A_c \frac{k_c}{k_{max}}} \quad (1)$$

where coefficient B_{1c} and A_c are the intercept and the slope of the curve in a semi-logarithmic plane. Coefficient B_{1c} was computed adopting, for a given value of the ratio k_c/k_{max}, a log-normal distribution of displacement around their mean value, whereas A_c was assumed to be equal to the slope of the median (50th-percentile) curve.

The upper-bound semi-empirical relationships were finally used to establish an equivalence between the corrected permanent displacements d and the seismic coefficient k to be used in LE pseudo-static analyses, so that k was calibrated against given threshold values of permanent displacements, d_y. In particular, equation (1) can be inverted to obtain, for given subsoil class, acceleration level and threshold displacement d_y, the ratio $\eta = k_c/k_{max}$ (figure 3): therefore, if the seismic coefficient $k = \eta \cdot k_{max}$ is used in a LE pseudo-static analysis of the wall and a safety factor $F_S = 1$ is obtained (i.e. limit conditions are attained), then a maximum permanent displacement $d = d_y$ can be expected. If, instead, a safety factor $F_S > 1$ is computed, then the critical seismic coefficient of the wall k_c is by definition greater than the adopted seismic coefficient k, and a maximum permanent displacement lower than the threshold value can be predicted, $d < d_y$. Different values of d_y can be adopted, depending on soil behaviour (e.g. ductile or brittle) and on the structures that can be involved by wall movements. Computed values of coefficient η are listed in tables 2 and 3 for threshold displacements for GRE walls corresponding to $d_y = 2$ and 5 cm, respectively. For $\eta < 0.10$ the minimum value $\eta = 0.10$ was assumed ($a_{max} = 0.35g$, subsoil

category E). As expected, coefficient η, that reduces a_{max}, increases for decreasing threshold displacements d_y, that is for a better required seismic performance, and for increasing peak acceleration a_{max}, that is for more intense earthquakes. The highest values of η are mostly computed for subsoil category C, while the lowest ones are obtained for subsoil category E.
In the proposed design procedure, this calibrated seismic coefficient is to be used to design the tensile strength of geosynthetic reinforcing layers T_T, imposing $k = k_c^{int}$. Then, the length of the reinforcing layers L can be selected so as to obtain a critical seismic coefficient related to external plastic mechanisms higher than the internal one, this meaning $k_c^{ext} > k_c^{int}$, in order to promote the activation of internal mechanisms during the seismic event. Imposing internal mechanisms to be triggered will strongly improve the performance of GRE walls, as already showed in previous studies and discussed in the following through the results of numerical analyses.

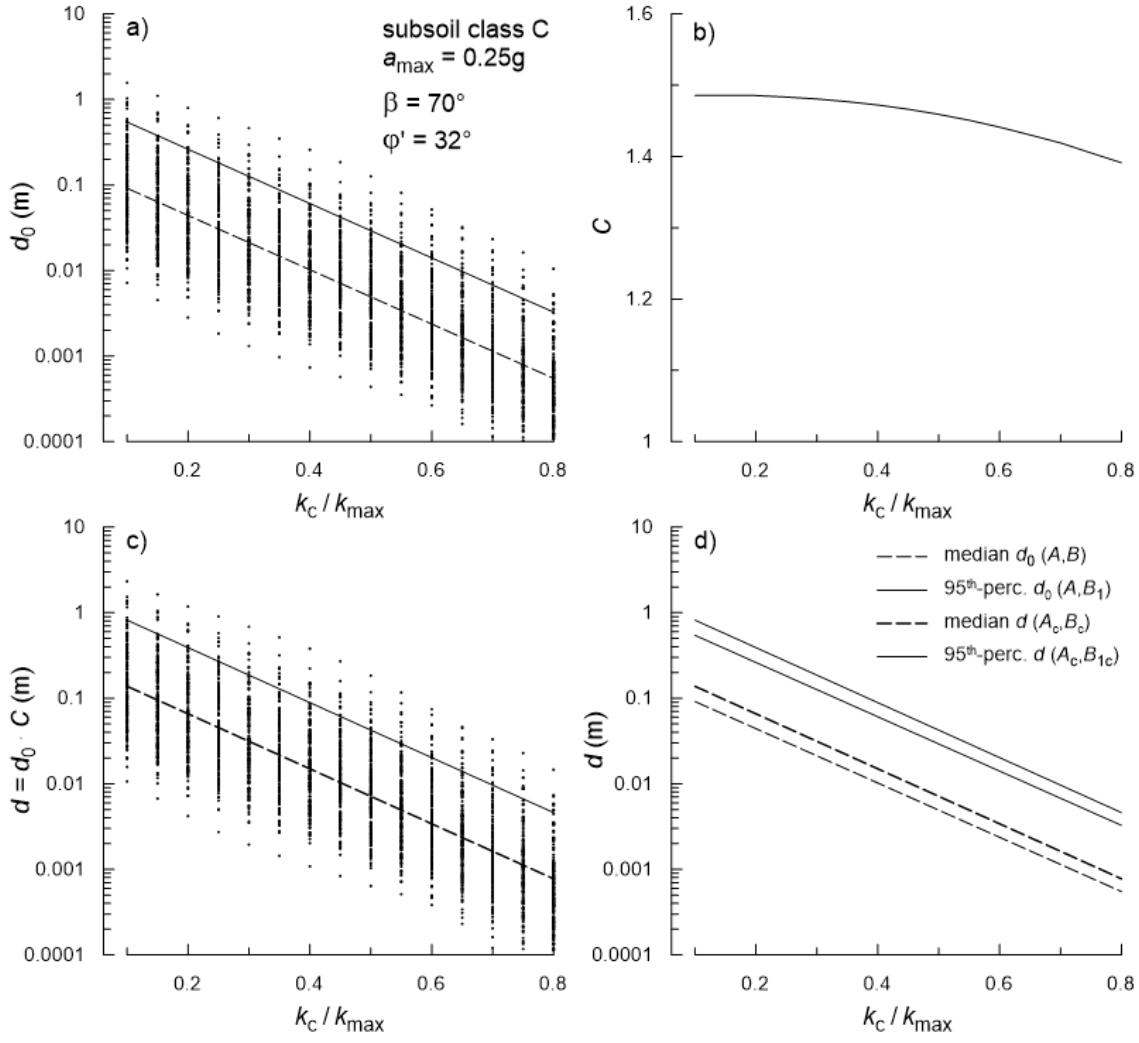

Figure 2. Evaluation of corrected permanent displacement d (subsoil category C, a_{max} = 0.25g) and comparison with displacement d_0.

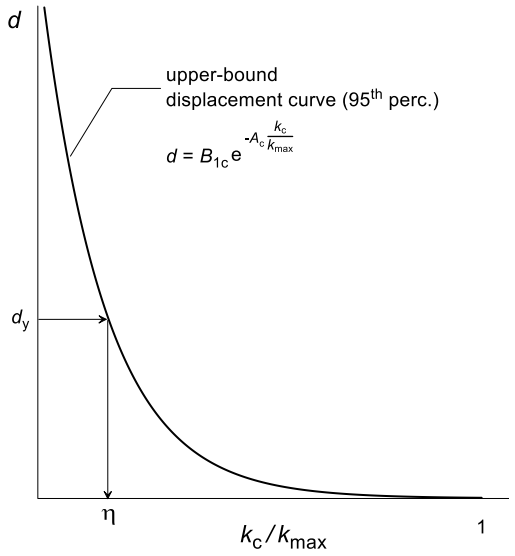

Figure 3. Scheme for calibrating seismic coefficient k as a function of the desired seismic performance.

Table 2. Values of η for d_y = 2 cm

a_{max}	Soil category				
(g)	A	B	C	D	E
0.35	0.61	0.58	0.67	0.57	0.50
0.25	0.52	0.53	0.60	0.55	0.43
0.15	0.43	0.45	0.52	0.52	0.33
0.05	0.28	0.32	0.38	0.49	0.20

Table 3. Values of η for d_y = 5 cm

a_{max}	Soil category				
(g)	A	B	C	D	E
0.35	0.50	0.45	0.55	0.46	0.38
0.25	0.40	0.40	0.48	0.44	0.31
0.15	0.31	0.33	0.40	0.41	0.20
0.05	0.16	0.20	0.26	0.38	0.10

3. Validation of the proposed design procedure

Effectiveness of designing GRE walls to trigger internal plastic mechanisms during intense seismic shakings is demonstrated in this paragraph, where the results of plane-strain nonlinear dynamic analyses, performed using the FD code FLAC v.5 [13] are discussed. Two different walls are considered in the analyses: the first represents a GRE wall for which an internal plastic mechanism is activated during earthquake loading, while the second is a conventional gravity wall that can only mobilise external plastic mechanisms during the seismic event. Characteristics and numerical modelling of these walls are presented first, together with the detection of plastic mechanisms: then, results of FD nonlinear dynamic analyses are discussed, showing the better seismic performance of the GRE wall.

3.1. Numerical modelling and detection of plastic mechanisms

Two idealised walls are considered, retaining the same backfill and founded on the same soil deposit, but activating internal and external plastic mechanisms, respectively (figure 4). The backfill is characterised by a height H = 15 m and a slope angle β = 80° relative to the horizontal.

The first wall (case 1 in figure 4) is a GRE wall designed, through the procedure previously described, to activate on purpose plastic mechanisms involving the geosynthetic reinforcing layers, this meaning to obtain an internal seismic coefficient, k_c^{int}, lower than the one related to external mechanisms, k_c^{ext}. This wall is characterised by 25 uniformly spaced geogrid layers (s = 0.6 m) and a length-to-height ratio L/H = 0.75 (L = 11.25 m). The fill is made by a coarse-grained soil with an angle of shearing resistance φ′ = 35°, while the foundation soil has φ′$_f$ = 28° and an effective cohesion c'_f = 10 kPa: both soils were characterised by a unit weight γ = 20 kN/m^3. Geogrid reinforcing layers are assigned a constant tensile strength T_T = 25 kN/m, a yield strain in the axial direction ε_y = 2 % and an infinite extensional ductility: it is worth mentioning that the latter is a primary hypothesis to simulate reinforcing layers ductile enough to provide a good seismic performance, as recently discussed in [8]. Resistance of soil-reinforcement contact was assumed to be purely attritive with a Mohr-Coulomb failure criterion and an angle φ′$_{s/GSY}$ = φ′ = 35°. For this wall, the following values of the internal and external critical coefficients are computed through the kinematic (upper-bound) theorem of limit analysis: k_c^{int} = 0.101 and k_c^{ext} = 0.196.

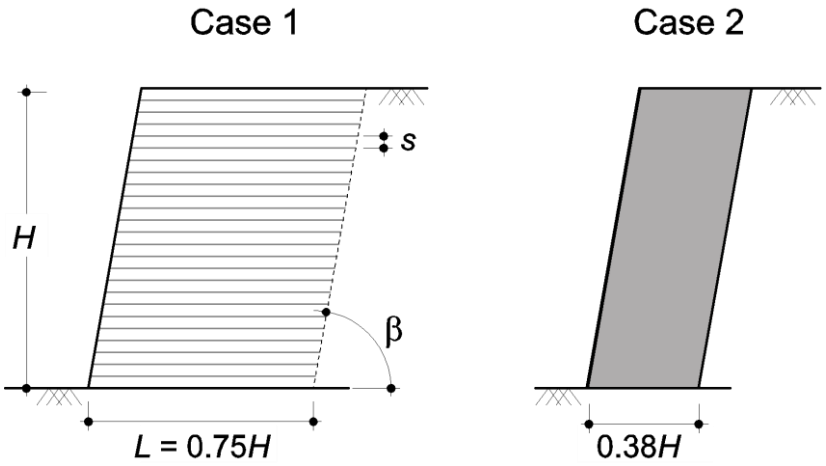

Figure 4. Layout of the two considered retaining walls.

The critical seismic coefficient k_c^{int} was also obtained by performing nonlinear pushover analyses using the code FLAC v.5 [13]. In these analyses, the horizontal component of volume forces, expressed as a fraction k_h of gravity g, was increased until numerical convergence could not be attained anymore. In these conditions well-defined internal plastic mechanisms were detected in the numerical model and the horizontal seismic coefficient k_h became, by definition, the critical seismic coefficient of the wall, $k_c = k_c^{int}$. In the numerical analyses soil behaviour was described using a linear elastic-perfectly plastic model with Mohr-Coulomb failure criterion and a zero dilatancy ($\psi = 0$). Geogrid reinforcing layers were modelled via FLAC *strip* elements, characterised by a linear elastic-perfectly plastic $T - \varepsilon_a$ relationship: therefore, axial (extensional) stiffness was only considered, as usually done for geosynthetic reinforcement. This would represent a polyester (PET) geogrid. Further details on the numerical model can be found in [8]. The value $k_c = k_c^{int} = 0.060$ was computed, that is lower than the one obtained through limit analysis. This result can be ascribed to two main reasons: the upper-bound solutions provided by the kinematic theorem of limit analysis and the different assumption made on the flow rule, associative in the upper-bound theorem ($\psi = \varphi'$) and non-associative in the FD analyses ($\psi = 0$).

The second wall (case 2) simulates a conventional gravity wall, characterised by the same seismic resistance of the GRE wall but related to an external plastic mechanism ($k_c^{ext}{}_{case\ 2} = k_c^{int}{}_{case\ 1}$). To this end the width of this wall, $L = 5.7$ m $= 0.38 \cdot H$, was selected to provide $k_c = k_c^{ext} = 0.060$, equal to the one already computed through the pseudo-static analyses for the GRE wall (case 1). In the FD numerical model, the gravity wall was simulated through a linear elastic material so as to inhibit any internal plastic mechanism.

Figure 5 shows the contours of shear strains at the end of the pseudo-static analyses, these identifying the plastic mechanisms of the two walls at hand. It is worth recalling that the values of the shear strains are not of interest when a failure mechanism is developed. For the GRE wall (case 1) two concurrent mechanisms are observed, both involving the reinforcing layers: the first one can be fairly approximated by a log-spiral rotational mechanism starting from the toe of the wall, while the second one is a two-block mechanisms passing through most of reinforcing layers and then approaching the backfill close to the top of the wall. Conversely, for the conventional gravity wall (case 2) any possible internal mechanism was prevented on purpose and therefore a fully external collapse mechanism is developed, this involving both foundation soil and backfill. Although characterised by the same seismic resistance ($k_c = 0.060$), the different deformation patterns occurring for the two walls will give rise to different seismic performance when subjected to the same seismic input, as it will be shown in the following.

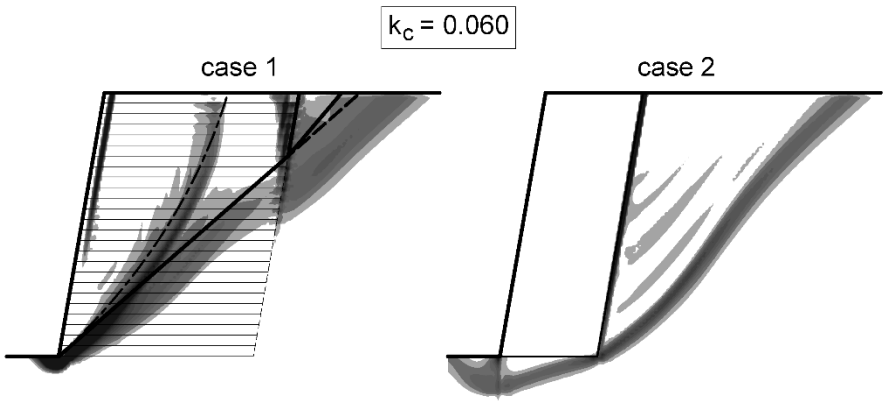

Figure 5. Plastic mechanisms of the walls (modified from [8]).

3.2. FD nonlinear dynamic analyses

Seismic performance of the walls was assessed by performing FD nonlinear dynamic analyses, adopting the same grid as the one used for the pushover analyses, just replacing the static boundary conditions with the FLAC free-field boundaries along the vertical sides while vertical displacements were still constrained at the base of the model, to simulate an infinitely rigid (i.e. fully-reflecting) bedrock. The seismic input was applied at the base of the grid through an acceleration time history.

In the dynamic analyses, soil behaviour was described via the hysteretic model available in the library of the FD code, coupled with Mohr-Coulomb failure criterion already recalled for the pseudo-static analyses. In the hysteretic model, the small-strain stiffness and the backbone curve are to be defined. To this end, parameters defining the dependency of small-strain shear modulus G_0 on the mean effective stress p' were selected to reproduce a typical small-strain stiffness of a medium plasticity sandy-silt for the foundation soils and a dense sand for the backfill: more details are given in [8]. Similarly, the backbone τ-γ curve, where τ and γ are the shear stress and strain respectively, was set to simulate shear modulus decay (G/G_0) and damping ratio increase (ξ) curves typically adopted for coarse-grained soils. These curves are plotted in figure 6: the obtained curves fairly resemble the ones provided by Seed and Idriss [14] and Vucetic and Dobry [15], except for the values of the hysteretic damping ratio obtained for high shear strains, $\gamma > 0.1$ %. A viscous damping ratio $D = 1$ % was added to reduce the numerical noise resulting from the hysteretic model at very low shear strains, where the hysteretic damping is close to zero: to this end, the Rayleigh formulation was adopted, selecting as central frequency the fundamental frequency of the soil deposit, $f = 1.02$ Hz.

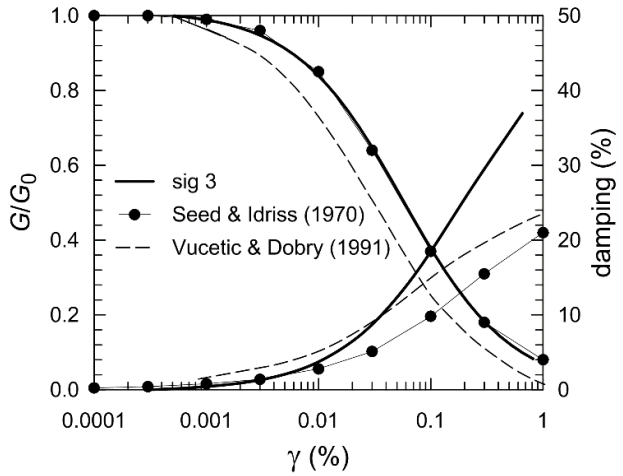

Figure 6. Modulus decay and equivalent damping ratio increase curves adopted in the numerical analyses (modified from [8]).

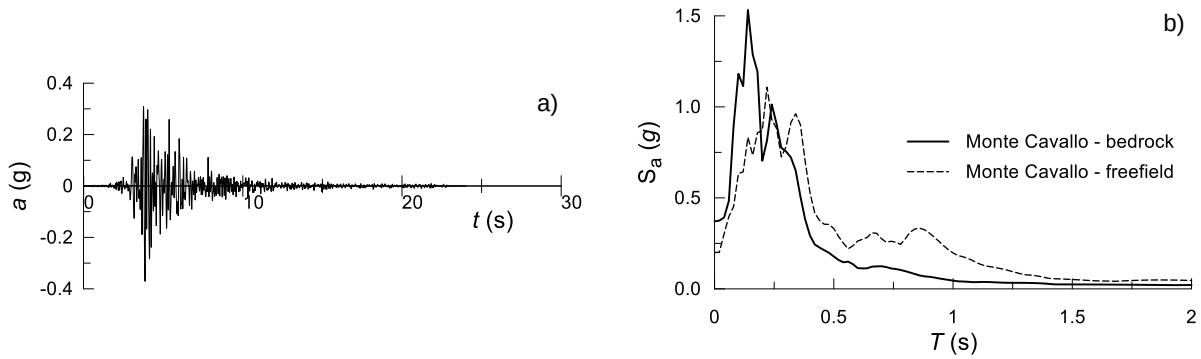

Figure 7. (a) Seismic input adopted in the analyses; (b) input and free-field acceleration spectra.

Both walls were subjected to the scaled (reduced in amplitude by a factor $F = 1.25$) horizontal acceleration time history recorded in Monte Cavallo during the October 2016 Central Italy earthquake (figure 7a), extracted from the updated version of the Italian seismic database [16].

This input motion is characterised by a peak acceleration $a_g = 0.37$g, Arias intensity $I_A = 0.75$ m/s, mean period $T_m = 0.20$ s [17] and a significant duration $T_D = 4.23$ s [18]. To comply with the adopted FD grid, the input was low-pass filtered ($f_{max} = 15$ Hz) and subjected to a quadratic baseline correction to obtain zero velocities and displacements at the end of the record. In figure 7b the 5 %-damped elastic acceleration spectrum obtained at ground surface in free-field conditions (that is, far enough from the wall) is compared with the one of the input motion: a noticeable reduction of spectral acceleration is observed at low periods ($T < 0.25$ s), this inducing a remarkable reduction of the peak acceleration $PGA = a_{max} = Sa(T = 0) = 0.20g$, while a strong amplification of motion occurs at higher periods ($T = 0.25 \div 2$ s).

Plastic mechanisms were actually triggered during the seismic event for both walls, as shown in figure 8, where the contours of shear strains at the end of the dynamic calculation phase are plotted. It is evident that the same plastic mechanisms as the ones obtained from the pseudo-static analyses (see figure 5) are mobilised. The deformation patterns associated to the different plastic mechanisms resulted in different permanent displacements developed at the end of the seismic event, that is in a different seismic performance of the walls.

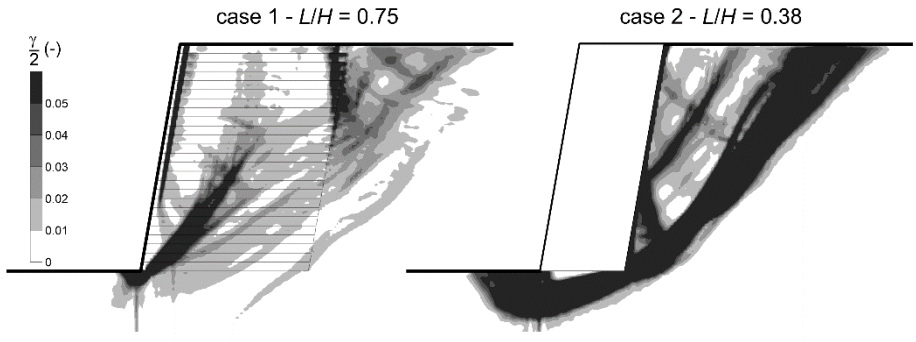

Figure 8. Contours of shear strains at the end of the dynamic calculation phase.

Figure 9 shows the time histories of the horizontal displacements at the base (B) and the top (T) of the wall façade, for both the walls under consideration. Displacements relative to that computed in free-field conditions, at the same relevant depth, are plotted in the figure. Values of $d_B = 0.26$ m ($d_B/H \approx 1.7$ %) and $d_B = 0.82$ m ($d_B/H \approx 5.5$ %) were computed at the base of the GRE and the

conventional gravity wall (CGW), respectively, with a ratio $d_{B,\,CGW}/d_{B,\,GRE} \approx 3.2$. Similarly, at the top of the wall façade displacements $d_T = 0.31$ m ($d_B/H \approx 2.0$ %) and $d_T = 0.56$ m ($d_B/H \approx 3.7$ %) are computed, this providing a ratio $d_{B,\,CGW}/d_{B,\,GRE} \approx 1.8$. Wu and Prakash [19] indicated values of $d_B/H \leq 2.0$ % as permissibile non-dimensional horizontal displacements: therefore, according to this criterion seismic performance of the GRE wall can be still deemed acceptable, while the one of the conventional gravity wall cannot.

Relative displacements computed at the base of the wall façade were also compared with those resulting from the semi-empirical relationships provided in [2] (figure 10). Indeed, these relationships can also be used to obtain a fair estimate of the order of magnitude of the expected displacements, as well as to calibrate the seismic coefficient k. For the case at hand, semi-empirical curves proposed for $a_{max} = 0.25$ g and subsoil class C are deemed the most appropriate to be used, with a ratio $k_c/k_{max} = 0.06/0.20 = 0.3$. It can be seen that the horizontal permanent displacement calculated for case 1 (GRE) wall plots close to the 95 % upper-bound curve, whereas the displacement computed for case 2 (conventional gravity) wall is much further from the curve and cannot be properly estimated with the proposed semi-empirical relationship. Moreover, the displacement resulting from the FD nonlinear dynamic analysis of the GRE wall falls into the computed range of displacements (grey-shaded area), computed through the parametric integration of the Italian seismic database using the rigid-block Newmark method, whereas the same does not hold for the conventional gravity wall.

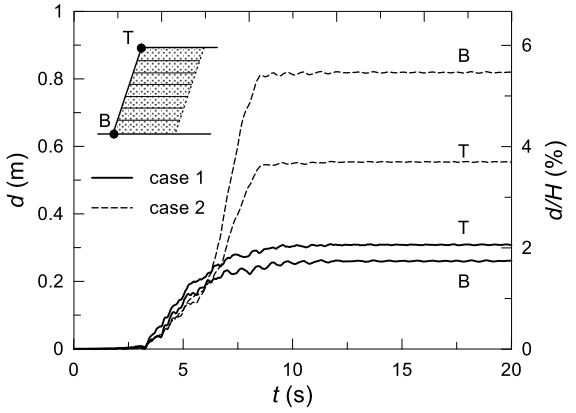

Figure 9. Time histories of horizontal displacements relative to free-field.

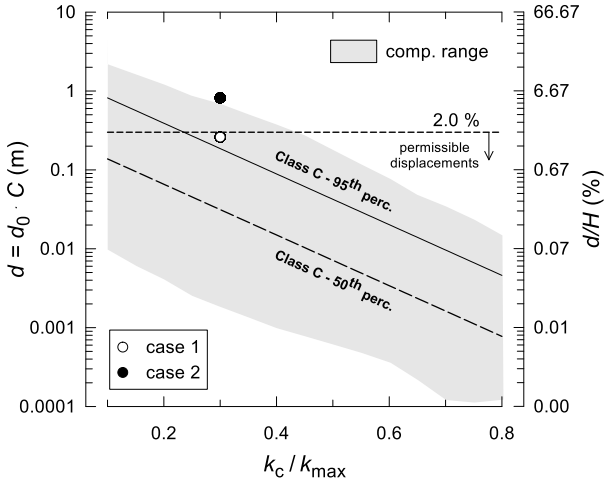

Figure 10. Comparison of permanent displacements obtained from dynamic analyses with those estimated with proposed semi-empirical relationship for $a_{max} = 0.25g$.

4. Concluding remarks

Seismic performance of geosynthetic-reinforced earth (GRE) retaining walls recently proved better than conventionally-designed retaining walls, thanks to the presence of reinforcing layers that redistribute seismic-induced strains into the reinforced zone. In this paper, a straightforward procedure recently developed to design GRE walls through the pseudo-static approach is firstly recalled. On the basis of upper-bound semi-empirical relationships linking permanent displacements to the ratio k_c/k_{max}, different values of the seismic coefficient k are provided as a function of the desired seismic performance of the wall, expressed by threshold displacement d_y (= 2 and 5 cm), earthquake intensity, quantified by the peak acceleration a_{max} (= 0.05, 0.15, 0.25 and 0.35g) and subsoil category (A, B, C, D, and E). In the proposed design procedure, it is suggested to design the GRE wall imposing the seismic coefficient k to be equal to the critical seismic coefficient related to an internal plastic mechanism, k_c^{int}, this being linked to the tensile strength of the reinforcing layers, T_T. The length of the reinforcing layers is then evaluated

so that the critical seismic coefficient associated to the external plastic mechanisms, k_c^{ext}, is higher than k_c^{int}: this to trigger internal plastic mechanisms during strong seismic events.

Effectiveness of the proposed procedure has been demonstrated showing that a GRE wall designed to activate internal plastic mechanisms during a severe earthquake actually behaves better than a conventionally-designed gravity wall, the latter triggering external plastic mechanisms only. To this end, FD nonlinear dynamic analyses were carried out, where the two walls were subjected to the same seismic record: the results showed that permanent displacements cumulated at wall façade for the GRE wall are much lower (up to about 70 %) than the ones computed for by the conventional gravity wall, this leading to a much better seismic performance.

It is useful recalling that conclusions drawn in this paper result from some underlying assumptions, these narrowing the range of applicability of the study. First, geosynthetic reinforcement layers are modelled as infinitely ductile: this is clearly a strong assumption, though quite realistic if bearing in mind the highly-ductile behaviour of geosynthetics compared to other materials (e.g. steel, glass, etc…). Second, the implicit hypothesis of infinitely flexible wall façade is made in this study, this being in principle suitable for wrap-around facing only, but neither for full-height rigid facing nor for modular blocks: nonetheless, concepts related to the better seismic performance of GRE walls still maintain.

References

[1] Paulay P and Priestley MJN 1992 *Seismic Design of Reinforced Concrete and Masonry Buildings* (New York: Wiley)
[2] Gaudio D, Masini L and Rampello S 2018 A performance-based approach to design reinforced-earth retaining walls *Geotext. Geomembr.* **46** pp 470 – 85
[3] Gaudio D, Masini L, Rampello S 2021 A Procedure to Design Geosynthetic-Reinforced Earth-Retaining Walls Under Seismic Loadings. In: Barla, M., Di Donna, A., Sterpi, D. (eds) Challenges and Innovations in Geomechanics. IACMAG 2021. Lecture Notes in Civil Engineering, **126** pp 300-8, Springer, Cham https://doi.org/10.1007/978-3-030-64518-2_36
[4] Yazdandoust M 2018 Seismic performance of soil-nailed using a 1g shaking table *Can. Geotech. J.* **55 pp** 1 – 18
[5] Gaudio D, Masini L and Rampello S 2018 Seismic performance of geosythetic-reinforced earth retaining walls subjected to strong ground motions *Proc. China-Europe Conf. Geotech. Eng. (Vienna)* (Springer Series in Geomechanics and Geoengineering 216849) pp 1474 – 78
[6] di Filippo G, Biondi G and Moraci N 2019 Seismic performance of geosynthetic-reinforced retaining walls: experimental tests vs numerical predictions *Proc. 7th Int. Conf. Earthq. Geotech. Eng. (Rome)* pp 2574 – 82
[7] Koseki J, Nakajima S, Tateyama M, Watanabe K, Shinoda M 2009 Seismic performance of geosynthetic reinforced soil retaining walls and their performance-based design in Japan *Proc. 7th Int. Conf. on Perf. based Design in Earthq. Eng. (Tokio)* pp 149 – 61
[8] Masini L, Callisto L and Rampello S 2015 An interpretation of the seismic behaviour of reinforced-earth retaining structures *Géotechnique* **65** pp 349 – 58
[9] Newmark NM 1965 Effects of earthquakes on dams and embankments *Géotechnique* **15** pp 139 – 93
[10] Cardile G, Pisano M and Moraci N 2019 The influence of a cyclic loading history on soil-geogrid interaction under pullout condition *Geotext. Geomembr.* **47** pp 552 – 65
[11] Gaudio D, Rauseo R, Masini L and Rampello S 2020. Semi-empirical relationships to assess the seismic performance of slopes from an updated version of the Italian seismic database *Bull Earthquake Eng* **18** pp 6245–81 https://doi.org/10.1007/s10518-020-00937-6
[12] Ministero delle Infrastrutture 2018 Norme Tecniche per le Costruzioni *Gazzetta Ufficiale della Repubblica Italiana* **42** (Rome: Decreto Ministero Infrastrutture 17.01.2018)
[13] Itasca 2005 *fast Lagrangian analysis of Continua v. 5.0. User's manual* (Minneapolis: Itasca Consulting Group)

[14] Seed H B and Idriss I M 1970 *Soil moduli and damping factors for dynamic response analyses* Report No. EERC70-10 (Berkeley, California: Earthquake Engineering Reaearch Centre)
[15] Vucetic M and Dobry R 1991 Effect of soil plasticity on cyclic response *J. Geotech. Eng.* **117** (1) 89 – 107
[16] Luzi L, Puglia R, Russo E and ORFEUS WG5 2016 *Engineering strong motion database, version 1.0* Istituto di Geofisica e Vulcanologia, Observatories & Research Facilities for European Seismology https://doi.org/10.13127/ESM
[17] Rathje E M, Abrahamson N A and Bray J D 1998 Simplified frequency content estimates of earthquake ground motions *J. Geotech. Geoenviron. Eng.* **124** pp 150 – 9
[18] Trifunac M D and Brady A G 1975 A study on the duration of strong earthquake ground motion *Bull. Seismol. Soc. Am.* **65 pp** 581 – 626
[19] Wu Y and Prakash S 1996 On the seismic displacements of rigid retaining walls *ASCE Geotech. Special Publ.: Analysis and Design of Retaining Structures against Earthquakes ASCE* pp 21 – 37